Journal of Zhejiang University-SCIENCE A (Applied Physics & Engineering)
ISSN 1673-565X (Print); ISSN 1862-1775 (Online)
www.zju.edu.cn/jzus; www.springerlink.com
E-mail: jzus@zju.edu.cn

Load-carrying capacity and practical calculation method for hollow cylinder joints connected with H-shaped beams*

Hui WU[1], Bo-qing GAO[†‡2], Qiang CHEN[2]
([1]Finance and Economics of Zhejiang College, Hangzhou 310018, China)
([2]College of Civil Engineering and Architecture, Zhejiang University, Hangzhou 310058, China)
[†]E-mail: bqgao@zju.edu.cn

Received Aug. 10, 2011; Revision accepted Oct. 31, 2011; Crosschecked Feb. 13, 2012

Abstract: A type of hollow cylinder joints connected with H-shaped beams is proposed for spatial structures. Based on von Mises yield criterion and perfect elasto-plasticity model, a series of finite element models of the joints is established, in which the effect of geometric nonlinearity is taken into account. Then mechanical behavior and load-carrying capacity of the joints were investigated, which were subjected to axial load, in- and out-plane bending moments, and their combinations. The results show that the ultimate loads of the joints are determined by the maximum displacement. Furthermore, the case of one joint connected with multiple beams was discussed. Experiments on a set of typical full-scale joints were conducted to understand the structural behavior and the failure mechanism of joint, and also to validate the finite element models. Finally, the practical calculation method was established through finite elements analysis (FEA) results and numerical fitting. The results show that the joints are more ductile and materially economical than welded hollow spherical joints, and the practical calculation method can provide a reference for direct design and the revision of relevant design codes.

Key words: Hollow cylinder joints, H-shaped beams, Load-carrying capacity, Finite elements analysis (FEA), Practical calculation method
doi:10.1631/jzus.A1100128 **Document code:** A **CLC number:** TU393.3

1 Introduction

Members of spatial reticulated structures are connected with joints, which may determine the application prospect of the structures. Bolted spherical, welded hollow spherical and circular hollow section (CHS) joints are widely applied in spatial structures in China (Shen *et al*., 2010). With the rapid increase of hardware and software computational power (van der Vegte *et al*., 2010), a great effort has been made to investigate the static strength (Han and Liu, 2004; López *et al*., 2007; Gho and Yang, 2008; Xing, 2010; Qiu *et al*., 2011) and hysteretic behavior (Yin *et al*., 2009; Wang *et al*., 2010; Shao *et al*., 2011) of these joints. Bolted spherical joints are easy to handle and apply to the structures, but their rigidities and strength are relatively small (Kim *et al*., 2008), and diameters of the sphere are usually much greater than those of members, which causes material waste and architectural defects. Conversely, the application of CHS tubular joints is affected by the stress concentration (Lee *et al*., 2011).

The joints above are connected with CHS tubular members. For other sections, Kosteski *et al.* (2003) obtained yield loads of rectangular hollow sections (RHSs) joints from load-deformation curves. Dong *et al.* (2005a; 2005b; 2006) investigated spherical joints connected with square steel tubular, bearing axial load,

‡ Corresponding author
* Project supported by the National Natural Science Foundation of China (No. 51178414), and the Science Foundation of Zhejiang Province (No. Y1110438), China

in- and out-plane moment and their combinations. A number of experimental tests were conducted to evaluate the rotational stiffness and capacity of cylinder joints connected with square steel tubular (López *et al*., 2011).

In this paper, we present a type of welded hollow cylinder joints connected with H-shaped beams, and propose corresponding practical load-carrying capacity formula through finite elements analysis (FEA) and experiments.

2 Numerical analysis

2.1 Finite element model

Fig. 1 demonstrates the hollow cylinder joint connected with H-shaped steel beams in a Kiewitt single layer reticulated shell. Cover plates could be welded at the end of a hollow cylinder according to the load-carrying capacity need.

Since the mechanical performance of the joints is complex, it is necessary to find the key factors that determine the load-carrying capacity. Here, ANSYS is employed to analyze static behavior of the joints. Eight-node solid element (SOLID45) with perfect elasto-plasticity material model is applied to build the FEA models. The load was applied on the cross-section at the free ends of the beam. In this study, we considered axial load, in- and out-plane bending moments and their combinations. Q345 steel was adopted in the simulation, and the yield strength is f_y=345 MPa. Considering symmetry, a typical FEA model of the joint is shown in Fig. 2.

2.2 Failure criterion

Under axial force and moments, deformations of the joints increase gradually with the increase of load. The maximum displacement of the joints d_0 appears at point *A* when the beam is subjected to axial compression or *Y*-direction moment, and d_0 appears at point *B* when the beam is subjected to *Z*-direction moment.

Usually the first peak of load-displacement curve is taken as the load-carrying capacity criterion (Han and Liu, 2004; Xue and Zhang, 2009). However, no obvious peak can be found in the load-displacement curve of hollow cylinder joints (Fig. 3), even when the deformation is relatively large. So the load-carrying capacity is determined by d_0. Here we set d_0=*D*/200 (where *D* is the outer diameter of the cylinder) to be the failure criterion of the hollow cylinder joints, which is equal to the displacement of the welded hollow spherical joint in its strength ultimate state (Xue and Zhang, 2009).

2.3 Behavior of the joints subjected to axial load

Under axial forces, the stress in the connection zone of beam and joint is relatively high. As the load

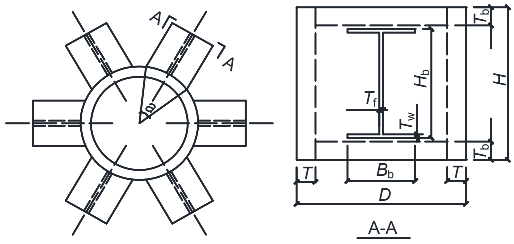

Fig. 1 Cylinder joint connected with six H-shaped beams
D: outer diameter of the cylinder; *T*: thickness of the cylinder; *H*: height of the cylinder; B_b: width of the H-shaped beams; H_b: height of the H-shaped beams; T_f: thickness of flange plate; T_w: thickness of web plate; T_b: thickness of cover plates; *α*: angle between the outer border of flange plate and the center of joint

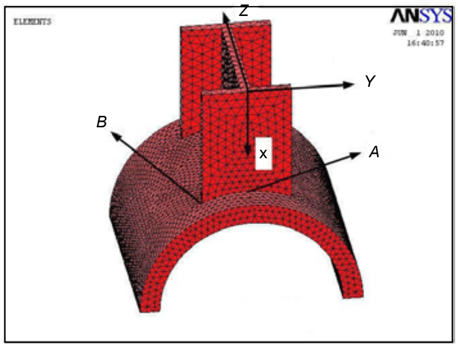

Fig. 2 FEA model of the joint without cover plates

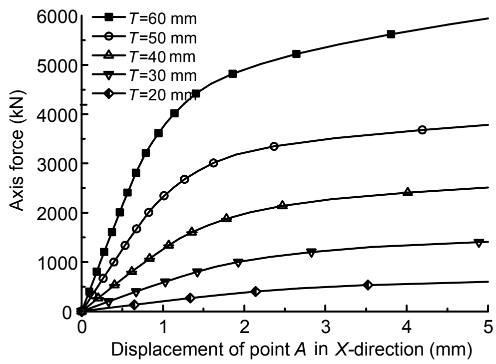

Fig. 3 Load-displacement curve of hollow cylinder joints with various thickness *T*

increases, a plastic zone first appears in the flange of the beam, and then diffuses to the whole connection zone, as shown in Fig. 4. Meanwhile, the stiffness of the joints decreases. When displacement in X-direction reaches d_0, the joint is considered reaching the ultimate state.

To calculate the ultimate load of joints subjected to axial load, we performed a number of FEA with different geometric parameters. According to preliminary analysis and the punching shear failure model (Dong *et al.*, 2005), the ultimate load is determined by the area of the punching shear surface, which is related to the thickness of the cylinder T, and width and height of the H-shaped beams B_b and H_b. Usually outer diameter of the cylinder D is determined by H_b, so we set B_b/D and T/D to be variable parameters.

The FEA results show that the ultimate tension load $F_{ux,t}$ is a little larger than the ultimate compression load $F_{ux,c}$. For safety and convenience, $F_{ux,c}$ is chosen to be the ultimate load, noted as $F_{ux,0}$. Fig. 5 shows the relationship between the ultimate axial load $F_{ux,0}$ and T/D, B_b/D when D=450 mm. Results of the cases where 200 mm<D<600 mm are similar. Through numerical fitting, we can obtain:

$$F_{ux,0}=\left(\alpha_0+\alpha_1\frac{T}{D}+\alpha_2\frac{B_b}{D}\right)f_y H_b T, \qquad (1)$$

where α_0=−0.32, α_1=6.76, α_2=0.55, and the range of parameter $1/30\leq T/D\leq 1/7.5$, $40°\leq\theta=2\arcsin(B_b/D)\leq 60°$.

Under axial load, the mechanical behavior of joints with cover plates is similar. When the joint reaches the limit state, almost the whole cover plates is plastic (Fig. 6). FEA results in Fig. 7 also show that cover plates enhance the joint, and the ultimate load, noted as F_{u0}, is proportional to thickness of the cover plates. Through numerical fitting, we can obtain:

$$F_{u0}=F_{ux,0}+2.7f_y B_b T_b. \qquad (2)$$

2.4 Behavior of the joints subjected to *Y*-direction moment

The ultimate moments in Y-direction of the joints without cover plates were obtained by FEA. The ultimate moment $M_{uy,0}$ of joints with different T (20 mm<T<60 mm) and D (200 mm<T<600 mm) are shown in Fig. 8. Through numerical fitting, the ultimate load is proportional to H_b, B_b, and T/D, and then we can obtain:

$$M_{uy,0}=\left(\alpha_0+\alpha_1\frac{T}{D}\right)^{\eta} f_y H_b B_b T, \qquad (3)$$

where α_0=−0.24, α_1=8.7, η=0.45, and the range of the geometric parameters is the same as shown in Eq. (1).

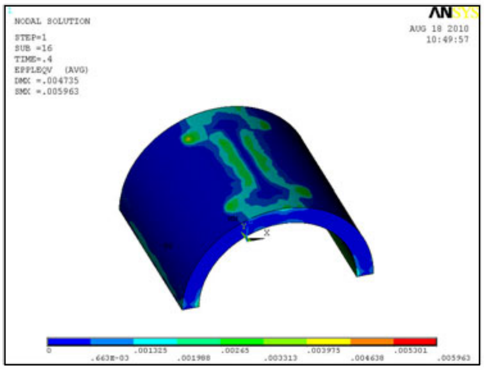

Fig. 4 Von Mises plastic strain of the joint without cover plates (*D*=450 mm, *T*=40 mm)

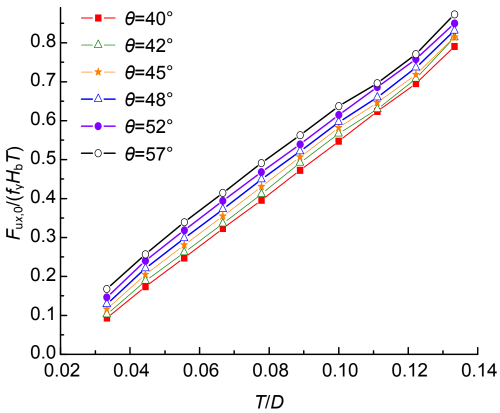

Fig. 5 Axial ultimate load of joints without cover plates (*D*=450 mm)

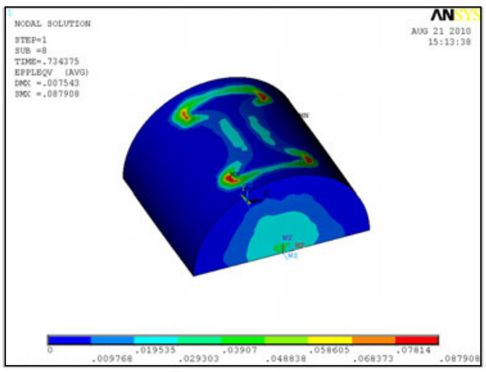

Fig. 6 Von Mises plastic strain of the joint with cover plates (*D*=450 mm, *T*=40 mm)

The ultimate moments of joints with cover plates, whose thickness T_b varies between 10 mm and T, are shown in Fig. 9. Through numerical fitting, we can obtain:

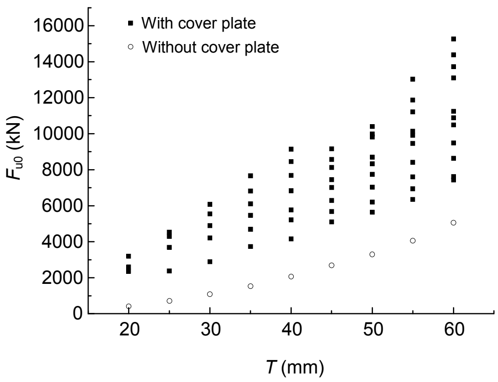

Fig. 7 Axial ultimate load of joints with cover plates
Different points with the same abscissa value stand for the results of models with different T_b

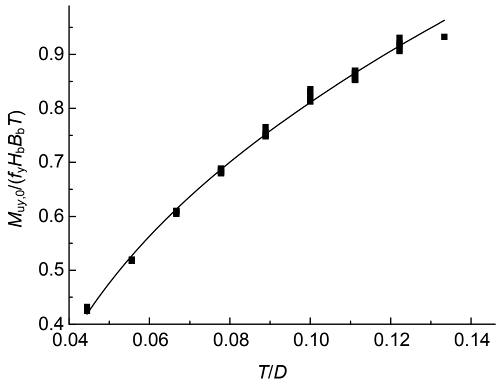

Fig. 8 Ultimate moment in *Y*-direction of joints without cover plates

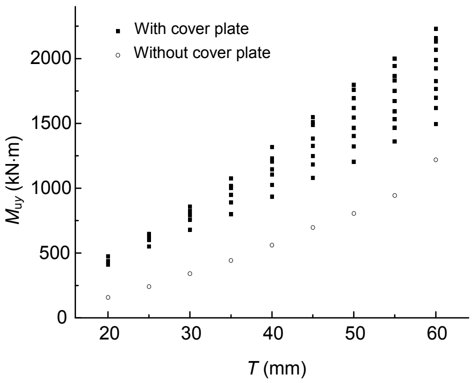

Fig. 9 Ultimate moment in *Y*-direction of joints with various *T* and T_b
Different points with the same abscissa value stand for the results of models with different T_b

$$M_{uy}=M_{uy,0}+0.5f_y H_b B_b T_b. \quad (4)$$

Further, the behavior of joints bearing combinations of axial load and *Y*-direction moment were analyzed. To obtain the ultimate axial load F_x and moment M_y, first two dimensionless indexes were introduced as follows:

$$\alpha_{M_y}=\frac{F_x}{F_{ux}},\ \beta_{M_y}=\frac{M_y}{M_{uy}},$$

where M_{uy}, F_{ux} are ultimate *Y*-direction moment and axial load, respectively when they are applied individually, and M_y, F_x are ultimate *Y*-direction moment and axial load, respectively when the joints are subjected to their combination. Then FEA models with three different joints (T=T_b=20, 40, 60 mm) were analyzed. The relationship between the two indexes, as shown in Fig. 10, is approximately independent of dimension.

By fitting, we can obtain:

$$\alpha_{M_y}+\beta_{M_y}=1. \quad (5)$$

2.5 Behavior of the joints subjected to *Z*-direction moment

Under *Z*-direction moment, the ultimate moment of joints without cover plates, noted as $M_{uz,0}$, is shown in Fig. 11. Through numerical fitting, we can obtain the ultimate moment $M_{uz,0}$:

$$M_{uz,0}=\left(\alpha_0+\alpha_1\frac{T}{D}\right)f_y B_b^2 T, \quad (6)$$

where α_0=−0.07, α_1=9.76.

The ultimate moment of joints with cover plates, whose thickness T_b varies between 10 mm and T, are shown in Fig. 12. Through numerical fitting, we can obtain:

$$M_{uz}=M_{uz,0}+0.3f_y B_b^2 T_b. \quad (7)$$

Further, the behavior of joints (T=T_b=20, 40, 60 mm) bearing combinations of axial load and *Z*-direction moment were analyzed. Also two dimensionless indexes were introduced as follows:

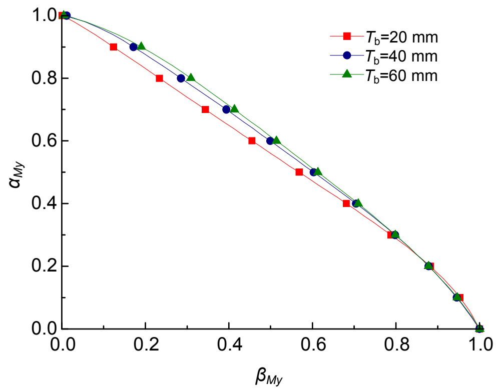

Fig. 10 Relationship between β_{M_y} and α_{M_y}

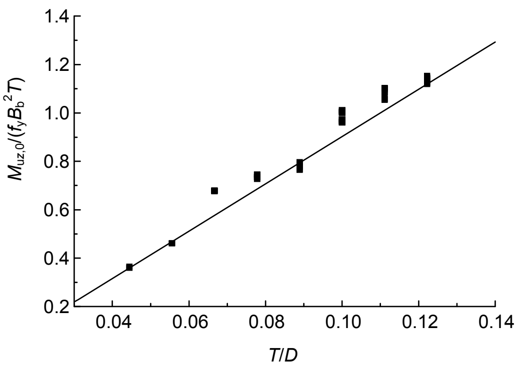

Fig. 11 Ultimate moment in *Z*-direction of joints without cover plates

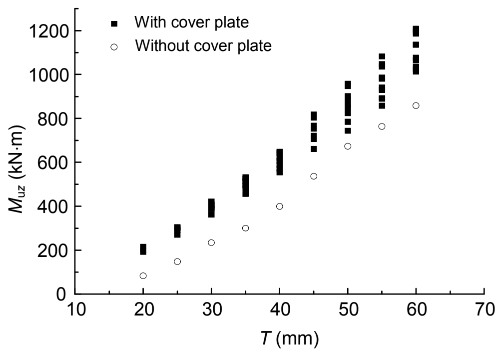

Fig. 12 Ultimate moment in *Z*-direction of joints with various *T* and T_b

Different points with the same abscissa value stand for the results of models with different T_b

$$\alpha_{M_z}=\frac{F_x}{F_{ux}},\ \beta_{M_z}=\frac{M_z}{M_{uz}},$$

where M_{uz}, F_{ux} are ultimate *Z*-direction moment and axial load, respectively when they are applied individually, and M_z, F_x are ultimate *Z*-direction moment and axial load, respectively when the joints are subjected to their combination. Then FEA models with three different joints (T=T_b=20, 40, 60 mm) were analyzed. The relationship between the two indexes is shown in Fig. 13. By fitting, we can obtain:

$$\alpha_{M_z}=(1-\beta_{M_z}^{1.2})^{1/1.2}. \tag{8}$$

2.6 Behavior of joints connected with multi members

For spatial structures, there are usually several beams attached to one single joint, and then the actual ultimate load is different. Yuan *et al.* (2007) proposed formulas for welded hollow spherical joints connected with multi members. Considering that member of spatial structures mainly bears axial force, here the moments are neglected. Fig. 14 shows a typical joint connected with three beams: the middle one, called key component beam, bears axial load F, and the other two, called neighborhood beams, bear F_1 and F_2 respectively.

Through FEA of various dimensional joints subjected to F and F_1=F_2, the ultimate axial load F_u is proportional to the value of F_1 or F_2, but independent of the thickness of the joint. Fig. 15 illustrates the relationship between F and F_1, in which positive

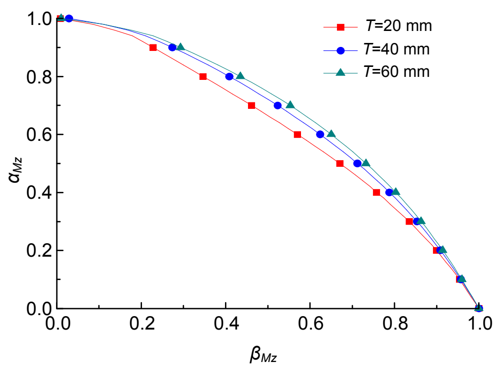

Fig. 13 Relationship between β_{M_z} and α_{M_z}

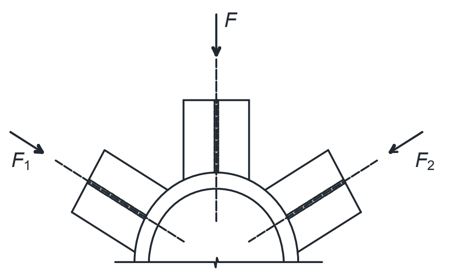

Fig. 14 A joint connected with three beams

value means compression load. Owing to punching shear failure, the ultimate compression load F_u decreases when neighboring beams are subjected to tension loads. Meanwhile, when $F_1=F_2=0$, F_u of joints connected with three beams are a little larger (8.0%, 10.3%, 4.7%, 4.0% for the four models, respectively) than those connected with only one beam, probably because neighborhood beams could slightly increase stiffness of the joints.

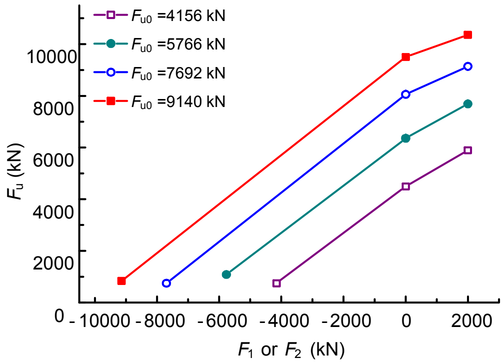

Fig. 15 Ultimate load when the neighborhood beams under various axial forces

Through numerical fitting, we can obtain the ultimate moment F_u as follows:

$$F_u=F_{u0}-\delta_1F_1-\delta_2F_2, \quad (9)$$

where δ_1 and δ_2 are neighborhood load influence coefficients, which equal to 0.45 if both F_1 (or F_2) and F are tension or compression load, otherwise equal to 0.

3 Experimental

To verify the accuracy and validity of the FEA results and proposed formulas, bidirectional eccentric compression experiments are performed on a 500 t hydraulic machine in the structure laboratory, Zhejiang University, China. The experimental rig is shown in Fig. 16. Pressure loads were applied to both ends of the specimen. Values of initial eccentric in Y- and Z-axis, noted as ε_Y and ε_Z respectively, were obtained by four strain gauges YB1–YB4 as shown in Fig. 17. The FEA results show that the maximum displacement appears at the edges of the flange in connection zone, so we set three dial indicators WY1–WY3 at the corners of the upper beam's flange and center of the under beam's flange.

Fig. 16 General view of the experiment

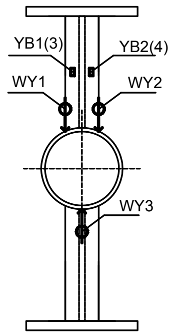

Fig. 17 Layout of strain gauges and dial indicators

The test scheme was gradual loading. The loading grade was set to be 1/5 of the load-carrying capacity calculated by Eqs. (1)–(8). To make the stress and strain stable, there was an interval between every two loading grades. The specimens were supposed to have failed when: (1) Turning point appears in load-displacement curves, or (2) $d_0=D/200$.

During the loading process, the maximum displacement d_0 was proportional to the load when the load was small. As loading continued to close to the ultimate load, d_0 increased fast and exceeded the specified value. Then the load decreased from the peak and the joint was considered to have failed. The load-displacement curve is illustrated in Fig. 18. As shown in Fig. 19, the hollow steel cylinder connected with H-shaped beam deformed significantly and compression buckling lead to the failure, which is consistent with the FEA results.

The experimental data are summarized in Table 1, where F_{simp}, F_{exp} and F_{FEA} refer to the result of proposed formulas, experiments and FEA, respectively. The FEA and simplified results generally agree with the test results, indicating that the FEA hypothesis is reasonable and the simplified formulas are proper for design.

4 Practical calculation method

According to results achieved above, a practical calculation method is proposed for load-carrying capacity of hollow cylinder joints connected with H-shaped beams. In- and out-plane moments and neighboring axial loads are taken into account. The procedure is

1. Obtain the key beam's axial load F_x, moments M_y, M_z, and the neighboring axial loads F_1, F_2. Here, the key beam means the beam bearing the maximum axial load.

2. Calculate the original ultimate axial load F_{u0} and in- and out-plane moments M_{uy}, M_{uz} through the following formulas:

$$\text{(a)}\ F_{u0}=\left(\alpha_0+\alpha_1\frac{T}{D}+\alpha_2\frac{B_b}{D}\right)f_y H_b T+2.7 f_y B_b T_b,$$

where α_0=−0.32, α_1=6.76, α_2=0.55;

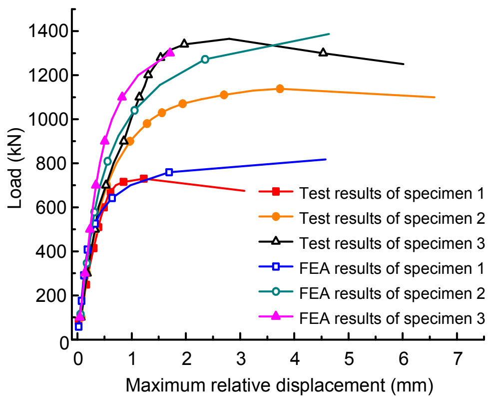

Fig. 18 Experimental and numerical results

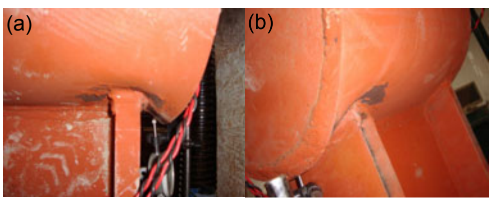

Fig. 19 Deformation of the connection zone

$$\text{(b)}\ M_{uy}=\left(\alpha_0+\alpha_1\frac{T}{D}\right)^{\eta} f_y H_b B_b T+0.5 f_y H_b B_b T_b,$$

where α_0=−0.24, α_1=8.7, η=0.45;

$$\text{(c)}\ M_{uz}=\left(\alpha_0+\alpha_1\frac{T}{D}\right) f_y B_b^2 T+0.3 f_y B_b^2 T_b,$$

where α_0=−0.07, α_1=9.76.

Then calculate the moment influence coefficients α_{M_y}, α_{M_z}:

$$\alpha_{M_y}=1-\frac{M_y}{M_{uy}},\quad \alpha_{M_z}=\left[1-\left(\frac{M_z}{M_{uz}}\right)^{1.2}\right]^{1/1.2}.$$

3. Finally, the ultimate load can be obtained when neighboring axial forces F_1=F_2:

$$F_u=\alpha_{M_y}\alpha_{M_z}(F_{u0}-\delta_1 F_1-\delta_2 F_2).$$

5 Conclusions

A type of hollow cylinder joints connected with H-shaped beams was proposed. Considering geometrical and material nonlinearities, parametric FEA was implemented by ANSYS to investigate the mechanical performance under axial load and in- and out-plane moments. Simplified formulas for load-carrying capacity of the joints were proposed, and formulas for joints subjected to axial force were verified by full-scale model experiments.

When axial load or moment is applied to the joints individually, the load-carrying capacity F_{ux} depends on thickness and diameter of the cylinder, thickness of cover plates and width and height of the beam. When the joints are subjected to combinations of axial load and moment, the ultimate load F_x will

Table 1 Load-carrying capacity of hollow cylinder joints under axial compression load

Specimen	D (mm)	T (mm)	T_b (mm)	H_b (mm)	B_b (mm)	ε_Y (mm)	ε_Z (mm)	F_{FEA} (kN)	F_{simp} (kN)	F_{exp} (kN)	F_{FEA}/F_{exp}	F_{simp}/F_{exp}
1	299	10	10	150	90	1	12	711	748	725	0.98	1.03
2	325	14	10	270	150	16	41	1170	979	1038	1.13	0.94
3	325	14	10	270	150	2	26	1286	1283	1300	0.99	0.99

decrease, and F_x/F_{ux} is independent of joint dimensions. When multi beams are attached to a single joint, the influence of neighboring members is proportional to the neighboring axial loads. Results of eccentric compression experiments agree well with the simplified formulas.

Reference

Dong, S.L., Tang, H.J., Zhao, Y., Fu, X.Y., Gu, L., 2005a. Load-carrying capacity and practical calculation method for welded hollow spherical joints subject to combined axial force and bending moment. *China Civil Engineering Journal*, **38**(1):21-30 (in Chinese).

Dong, S.L., Xing, L., Zhao, Y., Gu, L., Fu, X.Y., 2005b. Load-carrying capacity and practical calculation method of welded hollow spherical joints connected with square steel tubes. *Journal of Building Structures*, **26**(6):38-44 (in Chinese).

Dong, S.L., Xing, L., Zhao, Y., Gu, L., Fu, X.Y., 2006. Simplified theoretical solution and practical calculation method for welded hollow spherical joints of rectangular hollow section members. *China Civil Engineering Journal*, **39**(6):12-18 (in Chinese).

Gho, W.M., Yang, Y., 2008. Parametric equation for static strength of tubular circular hollow section joints with complete overlap of braces. *Journal of Structural Engineering*, **134**(3):393-401. [doi:10.1061/(ASCE)0733-9445(2008)134:3(393)]

Han, Q.H., Liu, X.L., 2004. Ultimate bearing capacity of the welded hollow spherical joints in spatial reticulated structures. *Engineering Structures*, **26**(1):73-82. [doi:10.1016/j.engstruct.2003.08.012]

Kim, Y.J., Lee, Y.H., Kim, H., 2008. Bending test of welded joints for single-layer latticed domes. *International Journal of Steel Structures*, **8**(4):357-367.

Kosteski, N., Packer, J.A., Puthli, R.S., 2003. Finite element method based yield load determination procedure for hollow structural section connections. *Journal of Constructional Steel Research*, **59**(4):453-471.

Lee, C.K., Chiew, S.P., Lie, S.T., Sopha, T., 2011. Comparison of fatigue performances of gapped and partially overlapped CHS K-joints. *Engineering Structures*, **33**(1): 44-52. [doi:10.1016/j.engstruct.2010.09.016]

López, A., Puente, I., Serna, M.A., 2007. Numerical model and experimental tests on single-layer latticed domes with semi-rigid joints. *Computers and Structures*, **85**(7-8): 360-374. [doi:10.1016/j.compstruc.2006.11.025]

López, A., Puente, I., Aizpurua, H., 2011. Experimental and analytical studies on the rotational stiffness of joints for single-layer structures. *Engineering Structures*, **33**(3): 731-737. [doi:10.1016/j.engstruct.2010.11.023]

Qiu, G.Z., Gong, J.H., Zhao, J.C., 2011. Parametric formulae for axial stiffness of CHS X-joints subjected to brace axial tension. *Journal of Zhejiang University-SCIENCE A (Applied Physics & Engineering)*, **12**(2):121-130. [doi:10.1631/jzus.A1000022]

Shao, Y.B., Li, T., Lie, S.T., Chiew, S.P., 2011. Hysteretic behaviour of square tubular T-joints with chord reinforcement under axial cyclic loading. *Journal of Constructional Steel Research*, **67**(1):140-149. [doi:10.1016/j.jcsr.2010.08.001]

Shen, Z.Y., Chen, Y.Y., Wang, W., Zhao, X.Z., 2010. Tubular structures in China: state of the art and applications. *Proceedings of the Institution of Civil Engineers-Structures and Buildings*, **163**(6):417-426. [doi:10.1680/stbu.2010.163.6.417]

van der Vegte, G.J., Wardenier, J., Puthli, R.S., 2010. FE analysis for welded hollow-section joints and bolted joints. *Proceedings of the Institution of Civil Engineers-Structures and Buildings*, **163**(6):427-437. [doi:10.1680/stbu.2010.163.6.427]

Wang, W., Chen, Y.Y., Meng, X.D., Leon, R.T., 2010. Behavior of thick-walled CHS X-joints under cyclic out-of-plane bending. *Journal of Constructional Steel Research*, **66**(6):826-834. [doi:10.1016/j.jcsr.2010.01.014]

Xing, L., 2010. Load-carrying capacity and practical design method of welded hollow spherical joints in space latticed structures. *Advanced Steel Construction*, **6**(4):976-1000.

Xue, W.L., Zhang, Q.L., 2009. Destructive mechanism and experimental study of welded hollow spherical joints connected with circular steel tubes. *Journal of Building Structures*, **30**(5):155-161 (in Chinese).

Yin, Y., Han, Q.H., Bai, L.J., Yang, H.D., Wang, S.P., 2009. Experimental study on hysteretic behaviour of tubular N-joints. *Journal of Constructional Steel Research*, **65**(2): 326-334. [doi:10.1016/j.jcsr.2008.07.006]

Yuan, X.F., Peng, Z.L., Dong, S.L., 2007. Load-carrying capacity of welded hollow spherical joints subject to combined planar tri-directional axial force and bending moment. *Journal of Zhejiang University (Engineering Science)*, **41**(9):1436-1442 (in Chinese).